Il presente lavoro è stato pubblicato su Journal of Chromatography A, 1477 (2016) 47–55
con doi https://doi.org/10.1016/j.chroma.2016.11.048

#

Journal of Chromatography A, 1477 (2016) 47–55

Title:

Hydrophilic interaction and reversed phase mixed-mode liquid chromatography coupled to high resolution tandem mass spectrometry for polar lipids analysis

Sara Granafei[1], Pietro Azzone[1], Alessandro Spinelli[1], Ilario Losito[1,2], Francesco Palmisano[1,2], Tommaso R.I. Cataldi[1,2]*

[1]Dipartimento di Chimica and [2]Centro di Ricerca Interdipartimentale S.M.A.R.T., Università degli Studi di Bari Aldo Moro, Campus Universitario, Via E. Orabona, 4 - 70126 Bari, Italy

Number of Figures: 5
Number of Tables: 1
Supplemental Material: Yes

Keywords: mixed-mode chromatography, serially coupled columns, phospholipids, hydrophilic, hydrophobic, polar lipids, tandem mass spectrometry.

* Author for correspondence, *email*: tommaso.cataldi@uniba.it

Abstract

A hydrophilic interaction liquid chromatography (HILIC) fused-core column (150 × 2.1 mm ID, 2.7 µm particle size) and a short reversed-phase liquid chromatography (RPLC) column (20 mm × 2.1 mm ID, 1.9 µm) were serially coupled to perform mixed-mode chromatography (MMC) on complex mixtures of phospholipids (PL). Mobile phase composition and gradient elution program were, preliminarily, optimized using a mixture of phosphatidylcholines (PC), phosphatidylethanolamines (PE), their corresponding lyso-forms (LPC and LPE), and sphingomyelins (SM). Thus a mixture of PC extracted from soybean was characterized by MMC coupled to electrospray ionization (ESI) high-resolution Fourier-transform mass spectrometry (FTMS) using an orbital trap analyzer. Several previously undiscovered PC, including positional isomers (i.e. 16:0/19:1 and 19:1/16:0) of PC 35:1 and skeletal isomers (i.e. 18:1/18:2 and 18:0/18:3) of PC 36:3 were identified. Therefore, high-resolution MS/MS spectra unveiled the occurrence of isomers for several overall side chain compositions. The proposed MMC-ESI-FTMS/MS approach revealed an unprecedented capability in disclosing complexity of an actual lipid extract, thus representing a very promising approach to lipidomics.

1. Introduction

Lipidomics investigation based on liquid chromatography-mass spectrometry (LC-MS) is a rapidly growing field, which has greatly benefited from the introduction of new MS analysers, featuring high mass resolution/accuracy [1–6], and novel LC technologies, enabling very selective and efficient separations with reduced analysis time and solvent consumption [7,8]. Lipidomics-related LC separations can be accomplished by (i) normal phase LC (NPLC), which typically leads to separation of lipids on the basis of their polar functionalities, (ii) hydrophobic interaction mode of reversed-phase LC (RPLC), that enables the separation of lipid species as a function of their lipophilic tails, and (iii) hydrophilic interaction liquid chromatography (HILIC), which can be a good alternative to RPLC for separating polar compounds [2,9–11]. Interestingly, HILIC combines the features of both NPLC and RPLC, as it employs polar stationary phases typical of NPLC, such as silica, and mobile phases typical of RPLC, such as solvent mixtures containing more than 50–70% acetonitrile, though with a reversed eluotropic strength [10,12].

The LC-MS coupling greatly helps to cope with several shortcomings occurring in the direct analysis by MS. Firstly, the chromatographic separation alleviates ionization suppression effects [13]. Secondly, the LC step could enables the separation of (intra- and/or inter-class) isobaric or isomeric PL, which, if co-eluted, would make MS identification ambiguous. However, some inherent limitations of each LC mode, potentially affecting MS detection, must be also accounted for. NPLC, for instance, is certainly suitable for phospholipids analysis, but the highly polar solvents typically employed possess low ionization efficiency thus negatively affecting the LC-MS coupling [8]. Conversely, RPLC uses MS compliant mobile phases, but partial or severe lipid co-elution is quite common especially for highly complex samples. HILIC, which is particularly effective in providing class

separation, should avoid the co-elution of isobars belonging to different lipid classes, yet intra-class lipid competition for ionization could remain [14]. Moreover, the co-elution of lipids, belonging to the same class, having molecular masses differing by 2 Da leads to the unavoidable superposition of spectra referred to the M+0 isotopologue of the target lipid and to the M+2 isotopologue related to the 2 Da lighter one, garbling the interpretation of MS/MS spectra.

To overcome these issues, two-dimensional (2D) high-performance liquid chromatography coupled to mass spectrometry has been suggested. Specifically, a 2D LC approach can be performed on-line [15,16] or off-line [17] and offers the chance to analyze complex lipid mixtures [16,18] using orthogonality in the separation mechanism operating in the two dimensions [19,20]. Among 2D approaches, comprehensive LCxLC is certainly the most promising, in spite of the higher instrumental complexity required [21]; note, however, that a partial loss of orthogonality has been experienced when using RPLCxRPLC [22] or HILICxHILIC [23]. A viable and instrumentally simpler alternative approach for analysing highly complex samples could be represented by mixed-mode chromatography (MMC) [24,25], potentially offering high selectivity, high sample loadings and speed [2,25,26]. MMC is typically performed by: (i) serial connection of two columns packed with different stationary phases (ii) use of a single column packed with two different stationary phases or (iii) use of special stationary phases, possessing ad-hoc designed functional groups displaying several domains (e.g. hydrophilic, hydrophobic, ionic) and then capable of combining orthogonal separation principles [25]. Two *in series* (tandem) columns, with no interface between them, is the simplest way to implement MMC, provided that mobile phase and/or gradient elution are compatible with both columns [25]. Since PL are characterized by a polar head (class specific) and by hydrophobic acyl chains, a suitable column combination

would be HILIC-RPLC, potentially capable of achieving between- and within-class separation, as demonstrated by HILIC-RPLC offline 2D-LC [17,27,28].

Few attempts to use MMC in lipid (mainly triacylglycerols – TAGs) analysis have been reported so far. Profiling of TAGs in plant oils on a mixed-mode phenyl-hexyl chromatographic column providing hydrophobic as well as π–π interactions has been described by Hu et al. [29]. TAGs separation could also be achieved by MMC on a single column packed with silver ion-modified octyl and sulfonic co-bonded silica, providing hydrophobic as well as complexation interactions [30]. Using a commercially available octadecylsilane column (end-capped with trimethylsilane moieties) and a mobile phase composed of methanol and isopropanol containing *para*-toluenesulfonic acid (as ion pairing agent) Lima and Synovec [31] demonstrated the separation of PL based on both non-polar fatty acid chain length and polar head group functionality. However, this approach cannot be classified as one of the three MMC modes above described so, to the best of our knowledge, no application of genuine MMC to phospholipidomics has been reported so far.

Starting from these considerations, an MMC approach based on the serial coupling of HILIC and RPLC columns, not requiring additional equipments (e.g. pumps, switching valves or T-pieces) has been developed for the separation of complex PL mixtures prior to MS detection. Its optimization and subsequent application to the characterization of a complex mixture of phosphatidylcholines is described here.

2. Materials and methods

2.1. Chemicals and standards

Water, methanol and acetonitrile (LC−MS grade), chloroform (HPLC grade) and ammonium acetate were obtained from Sigma-Aldrich (Milan, Italy). The standard L-α-

123 phosphatidylcholine from soybean (Sigma Aldrich) was dissolved in methanol and a solution
124 of 100 µg/mL was used for analysis. A standard mixture containing 10 µg/mL each of PE
125 18:0/22:6, PE 18:1/18:1, LPE 18:0, LPE 22:6, PC 16:0/20:4, PC 12:0/12:0, LPC 18:1 (Sigma
126 Aldrich) and 10 µg/mL of a SM standard mixture from chicken egg yolk was prepared. Note
127 that the lipid nomenclature described by Liebisch et al.[32] was adopted throughout this
128 paper.
129
130 **2.2. LC-MS instrumentations and operating conditions**
131 Ultra high performance (UHP) LC – high resolution MS was performed using an Ultimate
132 3000 UHPLC system (Thermo Scientific, Waltham, MA, USA) coupled to a Q-Exactive mass
133 spectrometer (Thermo Scientific, Waltham, MA, USA), including a quadrupole connected to
134 an Orbitrap analyzer. Sample injection (5 µL) was performed by a RS Autosampler (Thermo
135 Scientific, Waltham, MA, USA). The column effluent was transferred into the Q-Exactive
136 spectrometer through a heated electrospray ionization (HESI) interface. The main
137 electrospray and ion optics parameters were the following: sheath gas flow rate, 35 arbitrary
138 units (a.u.); auxiliary gas flow rate, 15 a.u.; spray voltage, ±3.5 kV (positive/negative
139 polarity); capillary temperature, 320 °C; S-Lens RF Level, 60 a.u. MS spectra were acquired in
140 the *m/z* range 120-1200, at a mass resolving power of 140000 (measured at *m/z* 200). The
141 Orbitrap fill-time was set to 200 ms and the automatic gain control (AGC) level was set to 2.5
142 $\times 10^6$. The Q-Exactive spectrometer was calibrated using a solution containing caffeine, the
143 MRFA peptide and Ultramark, provided by Thermo Scientific. Mass accuracy ranged between
144 0.15 and 0.16 ppm in positive polarity and between 0.43 and 0.74 ppm in negative polarity.
145 In order to retrieve molecular information on the separated PL, additional targeted-
146 MS^2 acquisitions were performed during each chromatographic run using a resolving power

of 70000 (at *m/z* 200), an Orbitrap fill-time of 100 ms and an AGC value of 5×10^5. The isolation window for precursor ions was 1.0 *m/z* unit wide, whereas the normalized collision energy (NCE) used for the higher energy collision dissociation (HCD) cell, was stepped at 15, 25 and 35 %. A stepwise fragmentation of the precursor ions (selected from an inclusion list of exact *m/z* values) was performed, then all generated fragments were collected and sent to the Orbitrap analyzer for single scan detection. All ions fragmentation (AIF) with multiple dissociation techniques, i.e. in source collision induced dissociation (sid) and HCD, providing MS and MS/MS data was also employed to increase the amount of retrievable information. AIF spectra were acquired using a NCE value of 35 % and the same resolving power, trap-fill time and AGC value adopted for MS acquisitions. The control of LC-MS instrumentation and the first processing of data were performed by the Xcalibur software 3.0.63 (Thermo Scientific).

RPLC, HILIC and MMC were tested separately. RPLC was performed at 30 °C on an Accucore Polar Premium C18 column (150 × 2.1 mm ID, 2.6 µm particle size) equipped with a Accucore Polar Premium C18 (10 × 2.1 mm ID) security guard cartridge (Thermo Scientific, Waltham, MA, USA), using the following elution program, based on water (solvent A) and methanol (solvent B), both containing 2.5 mmol/L of ammonium acetate: 0 − 3 min at 60% (v/v) solvent B, 3 − 5 min linear to 100% solvent B; 5 − 30 min isocratic, 30 − 35 min back to the initial composition, followed by 10 min equilibration time. The flow rate was 0.2 mL/min.

HILIC separations were performed at ambient temperature on a narrow-bore fused-core [33] Ascentis Express HILIC column (150 × 2.1 mm ID, 2.7 µm particle size) equipped with an Ascentis Express HILIC (5 × 2.1 mm ID) security guard cartridge (Supelco, Bellefonte, PA, USA), using the following elution program: 0 − 6 min, isocratic at 90% solvent B; 6 – 15 min, linear from 90% to 60% solvent B; 15 − 25 min, isocratic at 60% solvent B; 25 − 30 min,

linear to the initial composition, followed by 10 min equilibration time. The flow rate was 0.3 mL/min.

In the case of mixed-mode separations, performed at ambient temperature, the HILIC column described above was serially connected to a RP Hypersil GOLD aQ column (20 mm length, 2.1 mm i.d. and 1.9 µm particle size) by a Viper^{TM} fitting (150 mm length and 0.13 mm i.d), to ensure a low dead-volume. The elution program found to be the most effective, among several tested (*vide infra*), was the following: 0 - 2 min, isocratic at 97% solvent B; 2 – 2.5 min, linear to 85% solvent B; 2.5 – 9 min, isocratic at 85% solvent B; 9 – 9.2 min, linear to 100% solvent B; 9.2 – 12 min, isocratic at 100% solvent B; 12 – 23 min, linear to 50% solvent B; 23 – 30 min, isocratic at 50% solvent B; 30 – 30.2 min linear to 35% solvent B; 30.2 – 48 min, isocratic at 35% solvent B; 48 – 50 min, linear to 10% of solvent B and 90% of pure acetonitrile (solvent C); 50 – 55 min isocratic (washing step) at 10% solvent B and 90% C; 55 – 57 min, return to the initial composition, followed by 10 min equilibration time. The operating flow was 0.3 mL/min.

Raw data provided by the described LC-MS systems were imported, further elaborated and finally converted into figures by the SigmaPlot 11.0 software (Systat Software, Inc., London, UK). The ChemDraw Pro 8.0.3 software (CambridgeSoft Corporation, Cambridge, MA, USA) was employed to draw chemical structures.

3. Results and discussion

3.1. Tandem column HILIC-RPLC mixed-mode chromatography.

The main aim of MMC performed by a serial coupling of HILIC and RPLC columns was to retain, as much as possible, the HILIC class-based elution of polar lipids, meanwhile providing intraclass lipid separation through the hydrophobic interaction between side

195 acyl chains and the RP stationary phase. Typically, one of the main problems faced in
196 MMC of lipids is the poor retention of the most polar PL species (LPE and LPC) in the RP
197 column and band broadening of the most retained ones during the HILIC step. Based on
198 this, an appropriate evaluation of column dimensions, mobile phase composition and
199 gradient elution program was accomplished during this study. As a result, a fused-core
200 HILIC column with a conventional length (150 × 2.1 mm ID, 2.7 µm particle size) [12] was
201 finally connected to a 20 mm long RP column, packed with sub-2-µm particles to
202 increase both peak capacity and sensitivity. Longer RP columns, such as 50 and 100 mm
203 ones (having a 2.1 mm ID and packed with fused-core 2.7 µm particles) were not
204 suitable in terms of retention times, peak broadening and symmetry, especially for the
205 most retained species.

206 Therefore, the PL and SM mixture described in section 2.1 was used to adjust the
207 MMC separation conditions in terms of mobile phase composition and gradient elution
208 program. First, XIC (eXtracted Ion Current) chromatograms were retrieved from MS
209 experiments performed in AIF mode, using the following extraction windows: 196.0380
210 ± 0.0020, for PE and LPE; 224.0693 ± 0.0022, for PC and LPC, and 168.0431 ± 0.0017, for
211 PC, LPC and SM. The latter intervals were centered on *m/z* values related to specific
212 product ions of the different PL classes, under HCD-MS/MS conditions [11]. Besides the
213 HCD fragmentation at 35% of normalized collision energy (NCE), a preliminary in source
214 dissociation (sid), at 40 eV collision energy, was performed to enhance the generation of
215 class-diagnostic ions during AIF acquisitions.

216 Several gradient elution programs were evaluated to attain the most effective
217 class separation of PE, LPE, PC, LPC and SM (for some examples see Figures S1-S3 and
218 Tables S1-S3 in the Supplementary Material). The elution program already described in

section 2.2 was finally chosen as the one ensuring the best separation between the five PL classes. Moreover, three concentrations of ammonium acetate (1, 2.5, 5 mM) were evaluated attempting to improve chromatographic peak shape. Although peak symmetry increased on increasing the buffer concentration, the retention of PC was significantly decreased at 5 mM of ammonium acetate, thus 2.5 mM was chosen as a good compromise.

For the sake of comparison, XIC traces obtained by RPLC-ESI(-)FTMS (plots A, C and E) and MMC-ESI(-)FTMS (plots B, D and F) are reported in Figure 1. As previously found [8,34], RPLC led to a significant overlap of peaks related to PE, LPE, PC, LPC and SM classes, which are squeezed into a retention-time window between 10 and 20 min. Conversely, MMC led to a significant improvement in PL classes separation, thus contributing to reduce ionization suppression effects in the ESI source. Indeed, as shown in Figure 1, injecting the same sample a remarkable increase (one or even two orders of magnitude) in the signal intensity was observed passing from RPLC to MMC. An excellent repeatability (five consecutive runs) was also found for MMC with between-run retention time fluctuations never exceeding 15-20 s for e.g. PC 16:1/18:2, PC 16:0/18:1 and PC 18:0/18:1, eluting at 26.0, 35.7 and 47.0 min, respectively. These results are a tangible effect of gradient optimization that maintain the PL class retention order typical of HILIC almost unchanged, the only exception being the elution of LPC before SM, as inferred from plots D and F in Figure 1.

3.2. HILIC, RPLC and MMC of phosphatidylcholines.

The performance of the developed HILIC-RPLC MMC method (compared to pure HILIC and RPLC) in terms of number of detected species in a single PL class was evaluated by analyzing a commercially available L-α-phosphocholine standard from soybean. As an

example, the XIC chromatograms obtained, summing the extracted ion currents of PC 34:3, 36:3 and 36:4, are shown in Figure 2. The HILIC separation of these three species, each potentially encompassing several isomeric compounds, was limited and occurred in a very narrow retention-time window, as expected for lipids belonging to the same PL class [11,35]. Not surprisingly, PC 36:4 and 36:3 were slightly less retained than PC 34:3 (see panel A in Figure 2) due to the presence of longer acyl chains slightly increasing hydrophobicity. Plot B in the same figure shows the elution order observed in RPLC. In this case PC 36:3 was more retained than PC 36:4, due to the lower number of C=C bonds along the side chains, implying a slight increase in molecular hydrophobicity. Conversely, PC 34:3 was almost co-eluted with PC 36:3. As apparent from panel C in Figure 2, the best separation was achieved using MMC, since also PC 36:3 and 34:3 could be distinctly recognized, in spite of their skewed peaks and limited resolution.

The unexpected presence of a lysophosphatidylcholine with an 18:2 residual acyl chain in the analyzed sample, enabled a comparison between HILIC, RPLC and MMC also for the LPC class, as shown in Figure 3. Both regioisomers of LPC 18:2 were well resolved using HILIC (Figure 3A) in agreement with previous investigations [11,36]. MS/MS data [11] clarified that the sn_1 regioisomer (i.e., LPC 0:0/18:2 missing the acyl chain on the sn_1 position of glycerol) was less retained than the sn_2 one (LPC 18:2/0:0). Resolution was kept nearly unchanged switching from HILIC to MMC (see Figure 3C), whereas it was definitely poor under RPLC conditions (see Figure 3B).

3.3. MMC-ESI-FTMS/MS of phosphatidylcholines

The examination of PC occurring in the standard mixture of soybean and separated using MMC was based on the synergy between their accurate *m/z* ratios and the

relevant HCD-FTMS/MS data. As already reported in the literature, PC were fragmented in negative ion mode as $[M\text{-}CH_3]^-$ ions [5,37,38], generated in the ESI source along with $[M+CH_3COO]^-$ and $[M+CH_3COOH\text{-}CH_3]^-$ ions, where M is the zwitterionic PC form. Typically, the $[M\text{-}CH_3]^-$ ion yield can be deliberately increased through in-source induced dissociation. Since the fragmentation of $[M\text{-}CH_3]^-$ ions is well-described in the literature and provides very useful structural information on PC [5,37–42], sid was systematically exploited before proceeding with the HCD-FTMS/MS fragmentations on soybean PC separated by MMC.

The structural characterization of PC was based mainly on the neutral loss of their fatty acyl chains as ketenes, a process reflecting the PC regiochemistry, since the abundance of the resulting ions follows the order $[M\text{-}H\text{-}R_2'CH{=}C{=}O]^- > [M\text{-}H\text{-}R_1'CH{=}C{=}O]^-$, where the subscripts 1 and 2 are related to the sn_1 and sn_2 positions of glycerol, respectively. Notably, under HCD conditions, the most abundant product ions corresponded to acyl chain carboxylates, that could be used to confirm the composition of each chain. Further signals resulting from $[M\text{-}CH_3]^-$ ions fragmentation were diagnostic of the head group, since they corresponded to the dehydrated glycerophosphocholine anion (*m/z* 224.07) and to the phosphocholine anion (*m/z* 168.04). The PC identified, using the described fragmentation patterns, after HILIC-, RPLC- or tandem column MMC-ESI-FTMS analysis of the L-α-phosphatidylcholine standard extracted from soybean are summarized in Table 1. In several cases the presence of two, or even three, isomers was established for a given *m/z* ratio, i.e. for a given overall side chain composition ranging from 32:0 to 38:4. Compared to RPLC [34,43], MMC generally led to a better separation between isomeric PC having the same overall side chain

composition (the only exceptions being the isomers of PC 33:2 and PC 33:1 - see Table 1).

The performance of the tandem column MMC can be appreciated by considering, as an example, data relevant to PC 34:3, that was found to correspond to two distinct species (numbered as 9a and 9b in Table 1). XIC traces obtained for PC 34:3 in positive mode using HILIC, RPLC and MMC are reported in plots A, B and C of Figure 4, respectively. The HCD-FTMS/MS spectra averaged under the peak(s) detected in each XIC trace are also shown, as insets. In the case of HILIC and RPLC, the MS/MS spectrum of the $[M\text{-}CH_3]^-$ ion (*m/z* 740.53) was, however, a superposition of the fragmentation patterns of both isomers, due to their remarkable degree of co-elution. Indeed, four carboxylate ions were clearly detected, at *m/z* 253.23, 255.23, 277.23, 279.23, and two of the four signals (expected to be generated from side chain losses as ketenes) were observed (see the insets of plots A and B in Figure 4). Specifically, the two most intense signals related to ketene losses (*m/z* 480.31 and 502.30) suggested that one of the isomers corresponded to PC 16:0/18:3 and the RPLC XIC trace suggested that this was the species labelled as 9b (see plot B in Figure 4). This hypothesis was clearly confirmed by the distinct MS/MS spectrum obtained for species 9b when using MMC. Moreover, thanks to the complete chromatographic separation enabled by this approach, in spite of the slight peak tailing (see panel C in Figure 4), also isomer 9a could be easily recognized, as PC 16:1/18:2.

A further example of the significant improvement in chromatographic selectivity achieved by MMC is described in Figure 5, where XIC traces for PC 36:3 arising from positive ion HILIC-, RPLC- and MMC-ESI-FTMS analyses are compared, along with the negative ion HCD-MS/MS spectra obtained in each case. Plot A in Figure 5 indicates that in HILIC mode an apparently single chromatographic peak was observed for PC 36:3; this species (labeled as

17a in Table 1) could be identified as PC 18:1/18:2 from the negative ion HCD-MS/MS spectrum, shown in the inset of Figure 5A. However, the same spectrum clearly suggested the presence of a co-eluting species, since two additional peaks (assignable as carboxylate anions and as ketene loss) were observed. Surprisingly, the additional peak arising from a ketene loss showed an odd *m/z* ratio (505.32), instead of an even one, whereas the signal assignable as carboxylate anion was detected at an even *m/z* value 280.24, instead of an odd one (see the expansions of the MS/MS spectrum in Figure 5A). These findings were explained by the co-elution of PC 36:4 and PC 36:3, occurring only under HILIC conditions (see Figure 2A). Indeed, the M+2 isotopologue of the $[M\text{-}CH_3]^-$ ion of PC 36:4 was fragmented in the HCD cell together with the M+0 isotopologue of the same ion for PC 36:3, since these ions are isobaric, at least at the mass resolution of the quadrupole adopted for precursor ion isolation. Conceivably, the fragmentation of the M+2 isotopologue of the $[M\text{-}CH_3]^-$ ion of a PC can, in principle, lead to a carboxylate with a *m/z* ratio 1 unit higher than that expected from the M+0 isotopologue, thus to an even *m/z* ratio, if one of the atoms present as a 1 Da heavier isotope in the precursor ion structure (i.e., a ^{13}C, ^{17}O or ^{2}H) is located in the carboxylate moiety. For the same reason a 1 Da heavier ketene loss could also occur, thus leading to a product ion with a *m/z* ratio 1 unit lower than that expected, i.e., to an ion with an odd *m/z* ratio.

As shown in Figure 5B, coelution was less severe in RPLC and, consequently, a RPLC-HCD-MS/MS spectrum not suffering from interference due to the M+2 isotopologue of PC 36:4 could be retrieved for PC 36:3 (see the inset of Figure 5B). Moreover, as shown in Figure 5B, both the XIC arising from positive ion FTMS analysis and the HCD-MS/MS spectrum suggested the presence of another isomer of PC 36:3, along with the established PC 18:1/18:2. The additional isomer, labeled as 17b in Table 1 and Figure 5, was characterized

by a weak but detectable signal related to a carboxylate ion at *m/z* 277.23, compatible with the presence of a 18:3 fatty chain, which, in turn, suggested the concurrent presence of a 18:0 chain. Unfortunately, the abundance of the 17b isomer was too low and, also due to competition with the 17a isomer, no signal due to ketene losses could be detected, thus the regiochemistry could not be assessed. However, a better, although not complete, separation of 17a and 17b isomers was achieved (see Figure 5C) by MMC. Consequently, a clean HCD-MS/MS spectrum could be retrieved also for isomer 17b (see the right inset in Figure 5C) and signals related to the 18:0 carboxylate (*m/z* 283.25) and to the ketene losses of both 18:0 and 18:3 chains (*m/z* 502.30 and 508.30, respectively) could be detected as well. More importantly, the abundance ratio related to the two ketene losses clearly suggested that isomer 17b corresponds to PC 18:0/18:3.

As described in Figures S5, S6 and S7 of the Supplementary Material, similar results were achieved during the characterization of PC 38:2, 36:2 and 35:2. In these cases, peak separation was somewhat improved passing from HILIC to RPLC (see plots B in Figures S5, S6 and S7), but two well separated, sometimes almost baseline-resolved, peaks were obtained only by MMC (see plots C in Figures S5, S6 and S7).

CONCLUSIONS

An MMC method, based on the serial coupling of HILIC and RPLC columns, was developed and successfully applied to the profiling and characterization of phospholipids in complex mixtures. Thanks to an appropriate choice of the gradient elution program, MMC enabled a separation between five different PL classes (i.e., PC, PE, LPC, LPE and SM) comparable to that usually achieved by HILIC. However, the chromatographic selectivity obtained by MMC for species belonging to the same phospholipid class was significantly greater than that

available with HILIC or RPLC separations. Once integrated with high-resolution MS and HCD-MS/MS, MMC enabled a much deeper characterization of a standard mixture of diacylic phosphatidylcholines, taken as a model for a complex mixture of PL belonging to the same class. Several previously undiscovered PC, in terms of side chain composition (with odd-numbered chains also identified) and/or regiochemistry, were characterized. Furthermore, MMC proved able to keep unaltered the very important regiochemistry-dependent separation of LPC typical of HILIC. These findings candidate MMC as a very promising and, at the same time, easy to develop analytical approaches for a refined characterization of complex samples in the lipidomics field.

Acknowledgment

This work was supported by the project PONa3_00395/1 “BIOSCIENZE & SALUTE (B&H)” of the *Italian Ministero per l'Istruzione, l'Università e la Ricerca* (MIUR), and through the research project PRIN 2012TLC44W_003.

This article contains supporting information.

References

[1] M.R. Wenk, The emerging field of lipidomics, Nat Rev Drug Discov. 4 (2005) 594–610. doi:10.1038/nrd1776.

[2] A. Carrasco-Pancorbo, N. Navas-Iglesias, L. Cuadros-Rodríguez, From lipid analysis towards lipidomics, a new challenge for the analytical chemistry of the 21st century. Part I: Modern lipid analysis, TrAC - Trends Anal. Chem. 28 (2009) 263–278. doi:10.1016/j.trac.2008.12.005.

[3] P.T. Ivanova, S.B. Milne, D.S. Myers, H.A. Brown, Lipidomics: a mass spectrometry based systems level analysis of cellular lipids, Curr. Opin. Chem. Biol. 13 (2009) 526–531. doi:10.1016/j.cbpa.2009.08.011.

[4] A. Shevchenko, K. Simons, Lipidomics: coming to grips with lipid diversity, Nat Rev Mol Cell Biol. 11 (2010) 593–598. doi:10.1038/nrm2934.

[5] X. Han, K. Yang, R.W. Gross, Multi-dimensional mass spectrometry-based shotgun lipidomics and novel strategies for lipidomic analyses, Mass Spectrom. Rev. 31 (2012) 134–178. doi:10.1002/mas.20342.

[6] B. Brügger, Lipidomics: analysis of the lipid composition of cells and subcellular organelles by electrospray ionization mass spectrometry., Annu. Rev. Biochem. 83 (2014) 79–98. doi:10.1146/annurev-biochem-060713-035324.

[7] M. Li, Z. Zhou, H. Nie, Y. Bai, H. Liu, Recent advances of chromatography and mass spectrometry in lipidomics, Anal. Bioanal. Chem. 399 (2011) 243–249. doi:10.1007/s00216-010-4327-y.

[8] T. Cajka, O. Fiehn, Comprehensive analysis of lipids in biological systems by liquid chromatography-mass spectrometry, TrAC - Trends Anal. Chem. 61 (2014) 192–206. doi:10.1016/j.trac.2014.04.017.

[9] M. Ståhlman, C.S. Ejsing, K. Tarasov, J. Perman, J. Borén, K. Ekroos, High-throughput shotgun lipidomics by quadrupole time-of-flight mass spectrometry, J. Chromatogr. B Anal. Technol. Biomed. Life Sci. 877 (2009) 2664–2672. doi:10.1016/j.jchromb.2009.02.037.

[10] B. Buszewski, S. Noga, Hydrophilic interaction liquid chromatography (HILIC)-a powerful separation technique, Anal. Bioanal. Chem. 402 (2012) 231–247. doi:10.1007/s00216-011-5308-5.

[11] S. Granafei, I. Losito, F. Palmisano, T.R.I. Cataldi, Identification of isobaric lyso-phosphatidylcholines in lipid extracts of gilthead sea bream (Sparus aurata) fillets by hydrophilic interaction liquid chromatography coupled to high-resolution Fourier-transform mass spectrometry, Anal. Bioanal. Chem. 407 (2015) 6391–6404. doi:10.1007/s00216-015-8671-9.

[12] P. Jandera, Stationary and mobile phases in hydrophilic interaction chromatography: A review, Anal. Chim. Acta. 692 (2011) 1–25. doi:10.1016/j.aca.2011.02.047.

[13] S. Pati, B. Nie, R.D. Arnold, B.S. Cummings, Extraction, chromatographic and mass spectrometric methods for lipid analysis, Biomed. Chromatogr. 30 (2016) 695–709. doi:10.1002/bmc.3683.

[14] S. Khoury, N. El Banna, S. Tfaili, P. Chaminade, A study of inter-species ion suppression in electrospray ionization-mass spectrometry of some phospholipid classes, Anal. Bioanal. Chem. 408 (2016) 1–13. doi:10.1007/s00216-015-9245-6.

[15] P.Q. Tranchida, P. Donato, G. Dugo, L. Mondello, P. Dugo, Comprehensive chromatographic methods for the analysis of lipids, TrAC - Trends Anal. Chem. 26 (2007) 191–205. doi:10.1016/j.trac.2007.01.006.

[16] M. Holčapek, M. Ovčačíková, M. Lísa, E. Cífková, T. Hájek, Continuous comprehensive two-dimensional liquid chromatography-electrospray ionization mass spectrometry of complex lipidomic samples., Anal. Bioanal. Chem. 407 (2015) 5033–43. doi:10.1007/s00216-015-8528-2.

[17] M. Lísa, E. Cífková, M. Holčapek, Lipidomic profiling of biological tissues using off-line two-dimensional high-performance liquid chromatography–mass spectrometry, J. Chromatogr. A. 1218 (2011) 5146–5156. doi:http://dx.doi.org/10.1016/j.chroma.2011.05.081.

[18] L. Mondello, M. Beccaria, P. Donato, F. Cacciola, G. Dugo, P. Dugo, Comprehensive two-dimensional liquid chromatography with evaporative light-scattering detection

for the analysis of triacylglycerols in Borago officinalis, J. Sep. Sci. 34 (2011) 688–692. doi:10.1002/jssc.201000843.

[19] P. Česla, T. Hájek, P. Jandera, Optimization of two-dimensional gradient liquid chromatography separations, J. Chromatogr. A. 1216 (2009) 3443–3457. doi:10.1016/j.chroma.2008.08.111.

[20] P. Jandera, P. Česla, T. Hájek, G. Vohralík, K. Vyňuchalová, J. Fischer, Optimization of separation in two-dimensional high-performance liquid chromatography by adjusting phase system selectivity and using programmed elution techniques, J. Chromatogr. A. 1189 (2008) 207–220. doi:10.1016/j.chroma.2007.11.053.

[21] I. François, K. Sandra, P. Sandra, Comprehensive liquid chromatography: Fundamental aspects and practical considerations-A review, Anal. Chim. Acta. 641 (2009) 14–31. doi:10.1016/j.aca.2009.03.041.

[22] P. Dugo, T. Kumm, B. Chiofalo, A. Cotroneo, L. Mondello, Separation of triacylglycerols in a complex lipidic matrix by using comprehensive two-dimensional liquid chromatography coupled with atmospheric pressure chemical ionization mass spectrometric detection., J. Sep. Sci. 29 (2006) 1146–1154. doi:10.1002/jssc.200500476.

[23] Y. Wang, X. Lu, G. Xu, Development of a comprehensive two-dimensional hydrophilic interaction chromatography/quadrupole time-of-flight mass spectrometry system and its application in separation and identification of saponins from Quillaja saponaria, J. Chromatogr. A. 1181 (2008) 51–59. doi:10.1016/j.chroma.2007.12.034.

[24] Pavel Jandera, Column Selection for Two-Dimensional LCxLC, LCGC North Am. 26 (2008) 72–82.

[25] Y. Yang, X. Geng, Mixed-mode chromatography and its applications to biopolymers, J. Chromatogr. A. 1218 (2011) 8813–8825. doi:10.1016/j.chroma.2011.10.009.

[26] T. Alvarez-Segura, C. Ortiz-Bolsico, J.R. Torres-Lapasió, M.C. García-Álvarez-Coque, Serial versus parallel columns using isocratic elution: A comparison of multi-column approaches in mono-dimensional liquid chromatography, J. Chromatogr. A. 1390 (2015) 95–102. doi:10.1016/j.chroma.2015.02.058.

[27] E. Cífková, M. Holčapek, M. Lísa, Nontargeted lipidomic characterization of porcine organs using hydrophilic interaction liquid chromatography and off-line two-dimensional liquid chromatography-electrospray ionization mass spectrometry, Lipids. 48 (2013) 915–928. doi:10.1007/s11745-013-3820-4.

[28] Y. Zhao, H.C.H. Law, Z. Zhang, H.C. Lam, Q. Quan, G. Li, I.K. Chu, Online coupling of hydrophilic interaction/strong cation exchange/reversed-phase liquid chromatography with porous graphitic carbon liquid chromatography for simultaneous proteomics and N-glycomics analysis, J. Chromatogr. A. 1415 (2015) 57–66. doi:10.1016/j.chroma.2015.08.017.

[29] N. Hu, F. Wei, X. Lv, L. Wu, X.Y. Dong, H. Chen, Profiling of triacylglycerols in plant oils by high-performance liquid chromatography-atmosphere pressure chemical ionization mass spectrometry using a novel mixed-mode column, J. Chromatogr. B Anal. Technol. Biomed. Life Sci. 972 (2014) 65–72. doi:10.1016/j.jchromb.2014.09.039.

[30] F. Wei, N. Hu, X. Lv, X.-Y. Dong, H. Chen, Quantitation of triacylglycerols in edible oils by off-line comprehensive two-dimensional liquid chromatography-atmospheric pressure chemical ionization mass spectrometry using a single column., J. Chromatogr. A. 1404 (2015) 60–71. doi:10.1016/j.chroma.2015.05.058.

[31] L.R. Lima, R.E. Synovec, Isocratic mixed mode liquid chromatographic separation of phospholipids with octadecylsilane-silica stationary phases, Talanta. 41 (1994) 581–588. doi:10.1016/0039-9140(94)80070-7.

[32] G. Liebisch, J.A. Vizcaino, H. Kofeler, M. Trotzmuller, W.J. Griffiths, G. Schmitz, F. Spener, M.J.O. Wakelam, Shorthand notation for lipid structures derived from mass spectrometry, J. Lipid Res. 54 (2013) 1523–1530. doi:10.1194/jlr.M033506.

[33] R. Hayes, A. Ahmed, T. Edge, H. Zhang, Core-shell particles: Preparation, fundamentals and applications in high performance liquid chromatography, J. Chromatogr. A. 1357 (2014) 36–52. doi:10.1016/j.chroma.2014.05.010.

[34] M. Narváez-Rivas, Q. Zhang, Comprehensive untargeted lipidomic analysis using core–shell C30 particle column and high field orbitrap mass spectrometer, J. Chromatogr. A. 1440 (2016) 123–134. doi:10.1016/j.chroma.2016.02.054.

[35] I. Losito, R. Patruno, E. Conte, T.R.I. Cataldi, F.M. Megli, F. Palmisano, Phospholipidomics of human blood microparticles, Anal. Chem. 85 (2013) 6405–6413. doi:10.1021/ac400829r.

[36] L. Facchini, I. Losito, C. Cianci, T.R.I. Cataldi, F. Palmisano, Structural characterization and profiling of lyso-phospholipids in fresh and in thermally stressed mussels by hydrophilic interaction liquid chromatography-electrospray ionization-Fourier transform mass spectrometry, Electrophoresis. (2016). doi:10.1002/elps.201500514.

[37] R.C. Murphy, Tandem Mass Spectrometry of Lipids, Royal Society of Chemistry, Cambridge, 2014. doi:10.1039/9781782626350.

[38] X. Han, Lipidomics Comprehensive Mass Spectrometry of Lipids, John Wiley & Sons, Inc., First edition, Hoboken, New Jersey 2016. doi:10.1088/1751-8113/44/8/085201.

[39] F.-F. Hsu, J. Turk, Electrospray ionization with low-energy collisionally activated dissociation tandem mass spectrometry of glycerophospholipids: mechanisms of fragmentation and structural characterization., J. Chromatogr. B. Analyt. Technol. Biomed. Life Sci. 877 (2009) 2673–2695. doi:10.1016/j.jchromb.2009.02.033.

[40] K. Ekroos, C.S. Ejsing, U. Bahr, M. Karas, K. Simons, A. Shevchenko, Charting molecular composition of phosphatidylcholines by fatty acid scanning and ion trap MS3 fragmentation., J. Lipid Res. 44 (2003) 2181–92. doi:10.1194/jlr.D300020-JLR200.

[41] T. Houjou, K. Yamatani, H. Nakanishi, M. Imagawa, T. Shimizu, R. Taguchi, Rapid and selective identification of molecular species in phosphatidylcholine and sphingomyelin by conditional neutral loss scanning and MS3, Rapid Commun. Mass Spectrom. 18 (2004) 3123–3130. doi:10.1002/rcm.1737.

[42] M. Pulfer, R.C. Murphy, Electrospray mass spectrometry of phospholipids, Mass Spectrom. Rev. 22 (2003) 332–364. doi:10.1002/mas.10061.

[43] C.W.N. Damen, G. Isaac, J. Langridge, T. Hankemeier, R.J. Vreeken, Enhanced lipid isomer separation in human plasma using reversed-phase UPLC with ion-mobility/high-resolution MS detection., J. Lipid Res. 55 (2014) 1772–1783. doi:10.1194/jlr.D047795.

[44] G. Liebisch, J.A. Vizcaíno, H. Köfeler, M. Trötzmüller, W.J. Griffiths, G. Schmitz, F. Spener, M.J.O. Wakelam, Shorthand notation for lipid structures derived from mass spectrometry., J. Lipid Res. 54 (2013) 1523–30. doi:10.1194/jlr.M033506.

Figure Captions

Figure 1. Extracted ion current (XIC) chromatograms obtained by RPC-ESI(-)-FTMS (A, C and E) and MMC-ESI(-)FTMS (B, D and F) analysis of the PE, LPE, PC, LPC and SM mixture described in Section 2.1. MS data were acquired in AIF mode. XICs were obtained using narrow windows centred on selected *m/z* values, corresponding to the following class-diagnostic ions: (A) and (B) *m/z* 196.0380 (PE and LPE); (C) and (D) *m/z* 224.0693 (PC and LPC); (E) and (F) *m/z* 168.0431 (PC, SM and LPC). The ESI-FTMS spectra were obtained coupling sid (collision energy of 40 eV) and HCD fragmentation (normalized collision energy of 35%).

Figure 2. XIC chromatograms obtained by summing ion currents at *m/z* 758.5694 (PC34:3), *m/z* 782.5694 (PC36 :4) and *m/z* 784.5851 (PC 36:3). A) HILIC-ESI-FTMS; B) RPC-ESI-FTMS and C) MMC-ESI-FTMS analysis, in positive ion mode, of the L-α-phosphocholine standard from soybean (Sigma-Aldrich). Peak assignement in the chromatographic trace was inferred from the underlying FTMS spectra.

Figure 3. XIC chromatograms obtained for LPC 18:2 after: A) HILIC-ESI-FTMS, B) RPC-ESI-FTMS and C) MMC-ESI-FTMS analysis, in positive ion mode, of the L-α-phosphocholine from soybean (Sigma-Aldrich). Chromatographic plots were obtained using the following *m/z* interval for ion current extraction: 520.3377 – 520.3419, centered on the *m/z* value of the $[M+H]^+$ ion (with M representing the zwitterionic PC). Peaks labelled as 24a and 24b refer to the sn_1 and sn_2 regioisomer of LPC 18:2, respectively (see Table 1), identified by MS/MS analysis on the respective $[M-H]^+$ ions.

Figure 4. XIC chromatograms obtained for PC 34:3 after the: A) HILIC-ESI-FTMS, B) RPC-ESI-FTMS and C) MMC-ESI-FTMS analysis, in positive ion mode, of the L-α-phosphocholine from soybean (Sigma-Aldrich). Ion current was extracted using the *m/z* window 756.5462-756.5614, centered on the *m/z* value of the $[M+H]^+$ ion. HCD-MS/MS spectra obtained for the $[M-CH_3]^-$ ion of PC 34:3 (*m/z* 740.5235) are shown in the insets. Generation of $[M-CH_3]^-$ ions was enhanced by sid at 40 eV. Assignement of peak 9a and 9b (see also Table 1) as PC 16:0/18:3 and PC 16:1/18:2, respectively, was based on the HCD-MS/MS spectra averaged under the corresponding, well resolved, peaks obtained using MMC (see plot C).

Figure 5. XIC chromatograms obtained for PC 36:3 after the: A) HILIC-ESI-FTMS, B) RPC-ESI-FTMS and C) MMC-ESI-FTMS analysis, in positive ion mode, of the L-α-phosphocholine from soybean (Sigma-Aldrich). Ion current was extracted using the *m/z* window 784.5812 – 784.5890, centered on the *m/z* value of the $[M+H]^+$ ion. HCD-MS/MS spectra obtained for the $[M-CH_3]^-$ ion of PC 36:3 (*m/z* 768.5549) are shown in the insets. Note that the chromatographic peaks shown in plot C) are referred to two isomeric forms of PC 36:3, numbered as 17a and 17b in Table 1. Assignement as PC 18:1/18:2 (17a) and PC 18:0/18:3 (17b), was based on the HCD-MS/MS spectra averaged under the corresponding peaks, well separated using MMC (see plot C).

Table 1. Overview of the chromatographic, mass spectrometric and structural information obtained for PC detected in a L-α-phosphatidylcholine standard extracted from soybean using single column HILIC or RPLC and tandem column MMC coupled to positive ion ESI-FTMS or to negative ion HCD-MS/MS.[a]

ID	Rel. Ab (%)	$[M+H]^+$	$[M\text{-}CH_3]^-$	Species	HILIC		RPLC		MMC	
					sn_1/sn_2[b]	Time (min)	sn_1/sn_2	Time (min)	sn_1/sn_2	Time (min)
PC 32:3	0.04	728.5225	712.4923	1	14:0/18:3	6.9	14:0/18:3	14.3	14:0/18:3	23.8
PC 32:2	0.36	730.5381	714.5079	2a	14:0/18:2	6.8	14:0/18:2	14.8	14:0/18:2	26.1
				2b	16:0_16:2	6.8	16:0_16:2	15.0	16:0_16:2	26.4
PC 32:1	0.11	732.5538	716.5236	3a	14:0_18:1	6.8	14:0_18:1	15.3	14:0_18:1	29.2
				3b	16:0/16:1	6.8	16:0/16:1	15.3	16:0/16:1	31.0
PC 32:0	0.29	734.5694	718.5392	4	16:0/16:0	6.8	16:0/16:0	16.2	16:0/16:0	39.4
PC 33:3	0.09	742.5381	726.5079	5a	15:1/18:2	6.6	15:1/18:2	14.5	15:1/18:2	24.3
				5b	-		-		15:0_18:3	24.9
PC 33:2	0.18	744.5538	728.5236	6a	15:0/18:2	6.7	15:0/18:2	15.00	15.0/18:2	27.9
				6b	-		16:0_17:2	15.00	16:0_17:2	27.9
				6c	-		15:1_18:1	15.00	15:1_18:1	27.9
PC 33:1	0.01	746.5694	730.5000	7a	16:0/17:1	6.7	16:0/17:1	15.8	16:0/17:1	32.0
				7b	15:0/18:1	6.7	15:0_18:1	15.8	15:0_18:1	32.0
PC 34:4	0.07	754.5381	738.5079	8a	16:2_18:2	6.6	16:2/18:2	14.3	16:2_18:2	22.8
				8b	16:1_18:3	6.6	18:3/16:1	14.3	18:3/16:1	24.0
PC 34:3	3.97	756.5538	740.5236	9a	16:1_18:2	6.6	16.1_18:2	14.7	16:1/18:2	26.0
				9b	16:0/18:3	6.6	16:0/18:3	15.0	16:0/18:3	28.3
PC 34:2	28.27	758.5694	742.5392	10	16:0/18:2	6.6	16:0/18:2	15.5	16:0/18:2	29.6
PC 34:1	2.87	760.5851	744.5549	11	16:0/18:1	6.6	16:0/18:1	16.2	16:0/18:1	35.7
PC 35:4	0.07	768.5540	752.6175	12	18:2/17:2	6.5	18:2/17:2	14.5	18:2/17:2	24.1
PC 35:2	0.13	772.5851	756.5549	13a	16:0_19:2	6.5	16:0/19:2	15.9	16:0_19:2	30.4
				13b	-		18:1/17:1	15.9	18:1_17:1	31.0
				13c	17:0/18:2	6.5	17:0/18:2	15.9	17:0/18:2	33.3
PC 35:1	0.01	774.6007	758.5705	14a	16:0/19:1	6.5	16:0/19:1	13.1	16:0/19:1	24.1
				14b	-		-		19:1/16.0	21.9
PC 36:6	0.86	778.5381	762.5079	15	18.3/18:3	6.5	18:3/18:3	14.1	18:3/18:2	21.9
PC 36:4	43.82	782.5694	766.5392	16a	18:2/18:2	6.4	18:2/18:2	15.0	18:2/18:2	25.0
				16b	18:3_18:1	6.4	18:3/18:1	15.0	18:3/18:1	26.1
PC 36:3	9.89	784.5851	768.5549	17a	18:1/18:2	6.3	18:1/18:2	15.4	18:1/18:2	29.3
				17b			18:0_18:3	15.4	18:0/18:3	31.9
PC 36:2	6.29	786.6007	770.5705	18a	18:0/18:2	6.3	18:0/18:2	16.6	18:0/18:2	36.3
				18b	18:1/18:1	6.3	18:1/18:1	16.6	18:1/18:1	34.1
PC 36:1	0.91	788.6164	772.5862	19	18:0/18:1	6.2	18:0/18:1	17.6	18:0/18:1	47.0
PC 37:3	0.37	798.5640	782.5705	20a	19:1/18:2	6.8	19:1/18:2	13.1	19:1/18:2	19.3
				20b	-		-		18:2/19:1	21.3
				20c	-		19:2/18:1	15.5	19:2_18:1	22.3
PC 38:4	0.20	810.6007	794.5705	21	20:2_18:2	6.2	20:2/18:2	15.7	20:2/18:2	29.1
PC 38:3	0.40	812.6164	796.5862	22a	20:1_18:2	6.2	20:1_18:2	16.4	20:1/18:2	35.4
				22b	-		20:0/18:3	16.4	20:0_18:3	40.1
PC 38:2	0.31	814.6320	798.6018	23a	20:0_18:2	6.1	20:0/18:2	17.8	20:0_18:2	49.2
				23b	-		-		20:1_18:1	44.0
LPC 18:2	0.47	520.3398	504.3085	24a	0:0/18:2	11.4	0:0/18:2	11.3	0:0/18:2	22.3
				24b	18:2/0:0	12.2	18:2/0:0	11.5	18:2/0:0	23.3

[a] Data are reported in the order of increasing *m/z* value; the most abundant species are written in bold character.
[b]The acyl chains at the sn_1/sn_2 positions are listed; in case where the regiochemistry could not be assessed by MS/MS data the chain compositions are separated by an underscore [44].

577 Figure 1
578

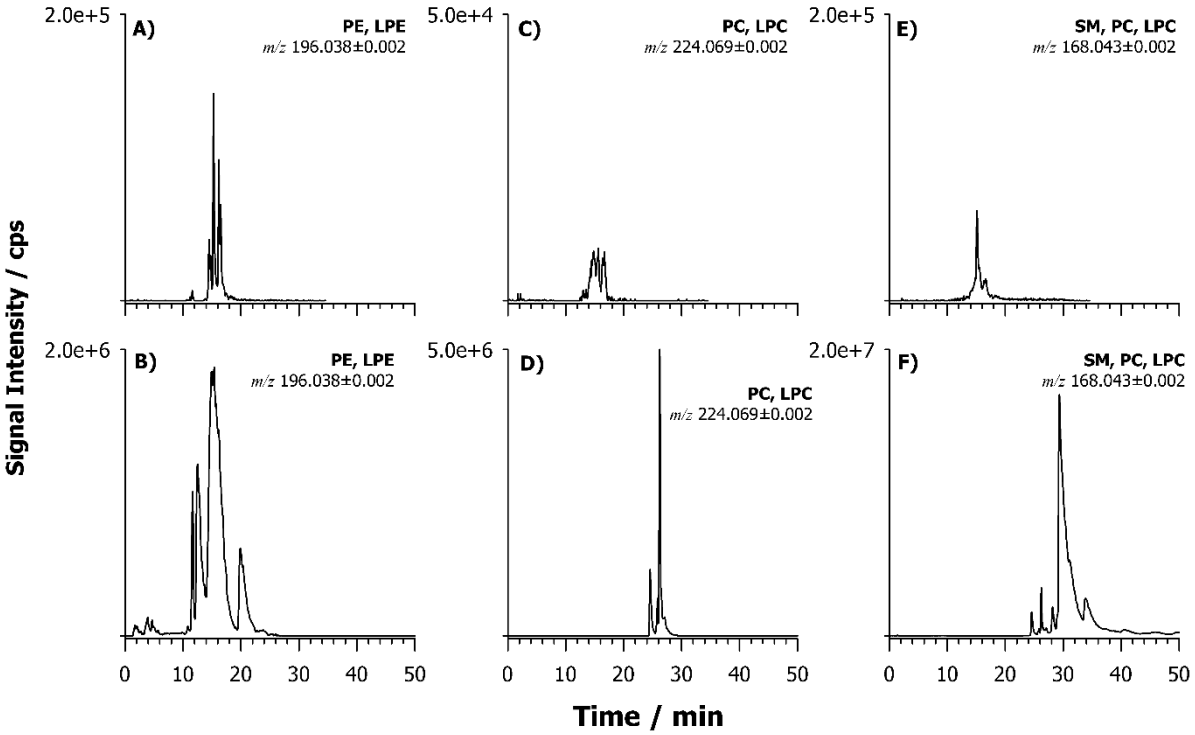

579
580

581 Figure 2
582

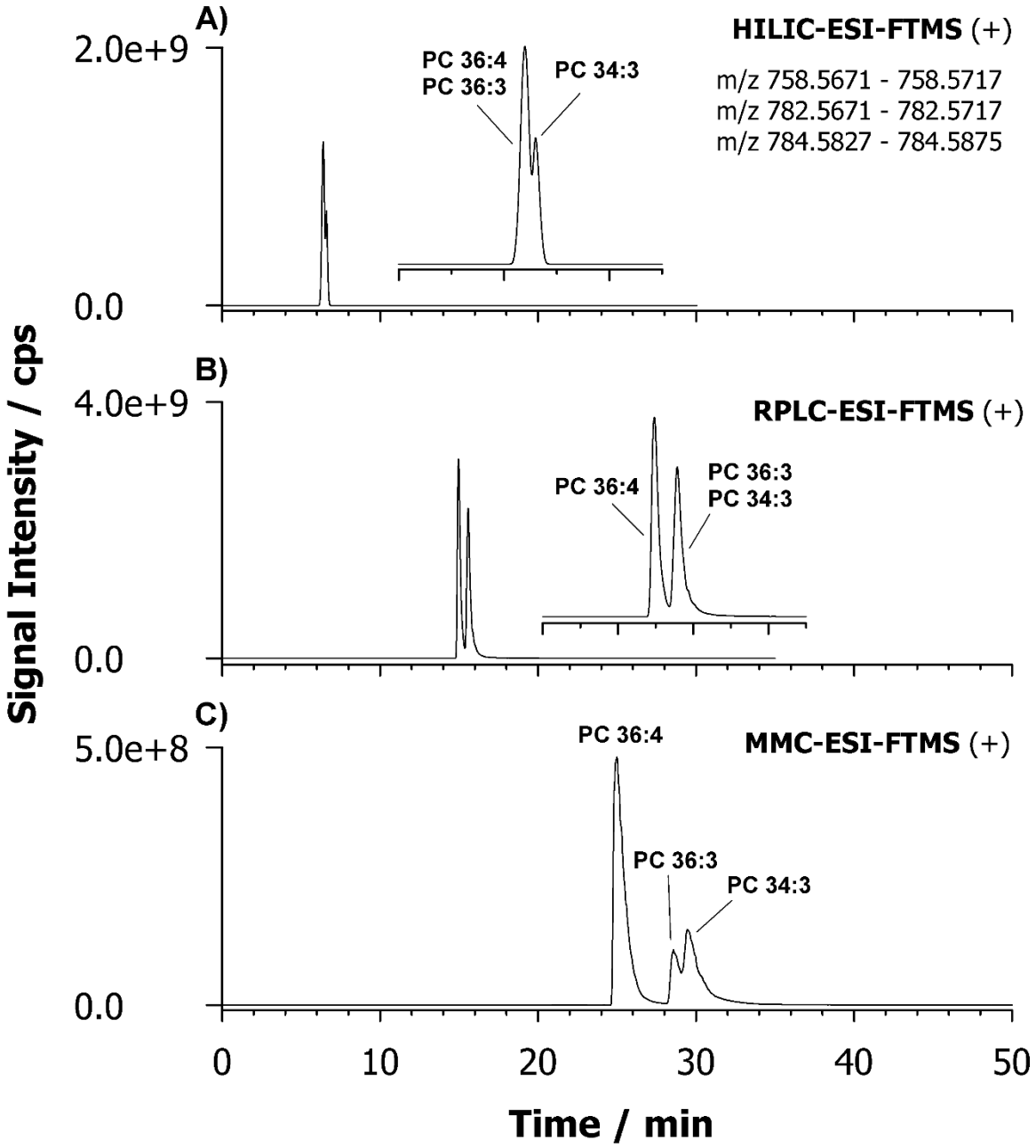

583
584
585

586 Figure 3
587

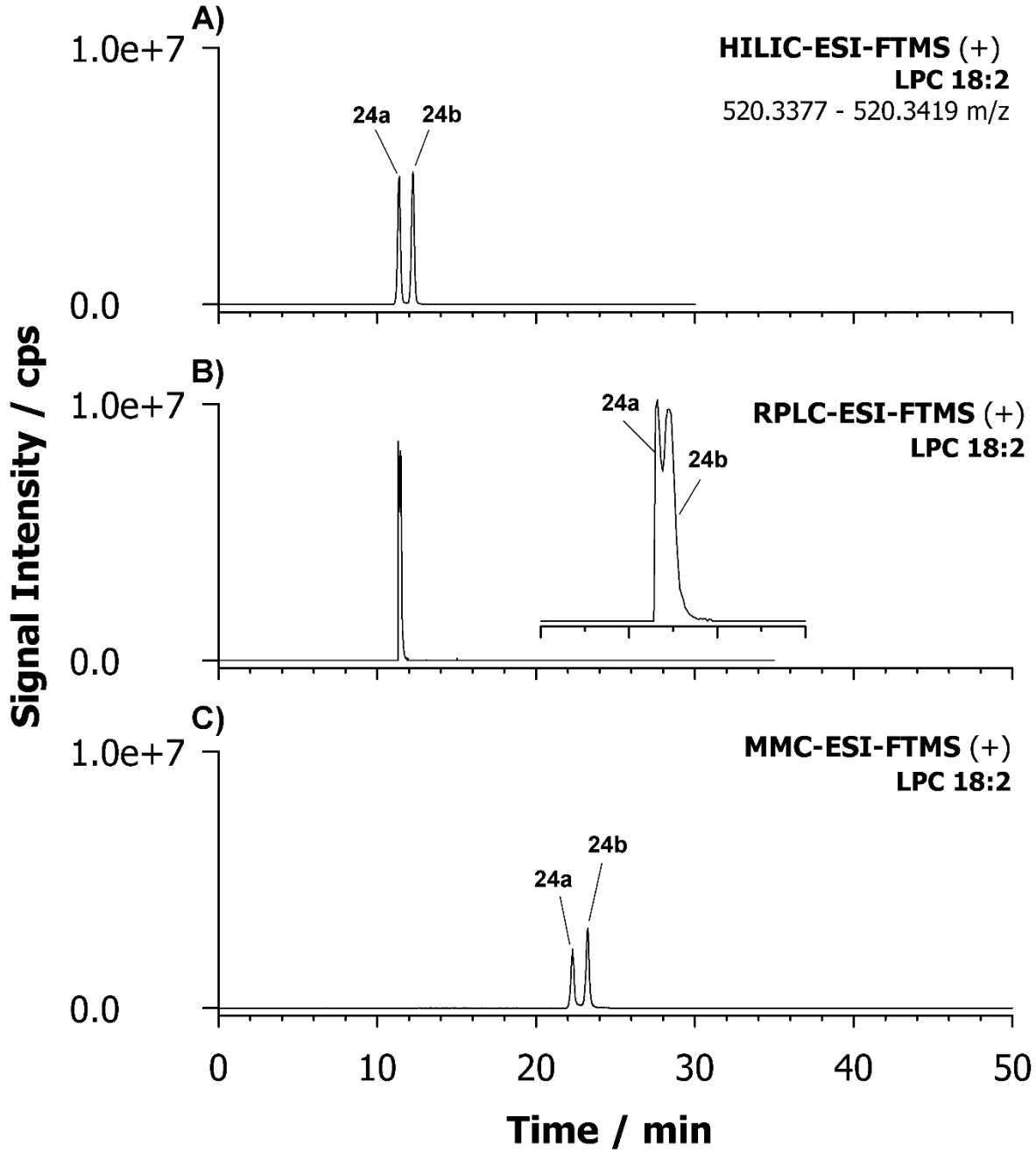

588
589
590
591

592 Figure 4

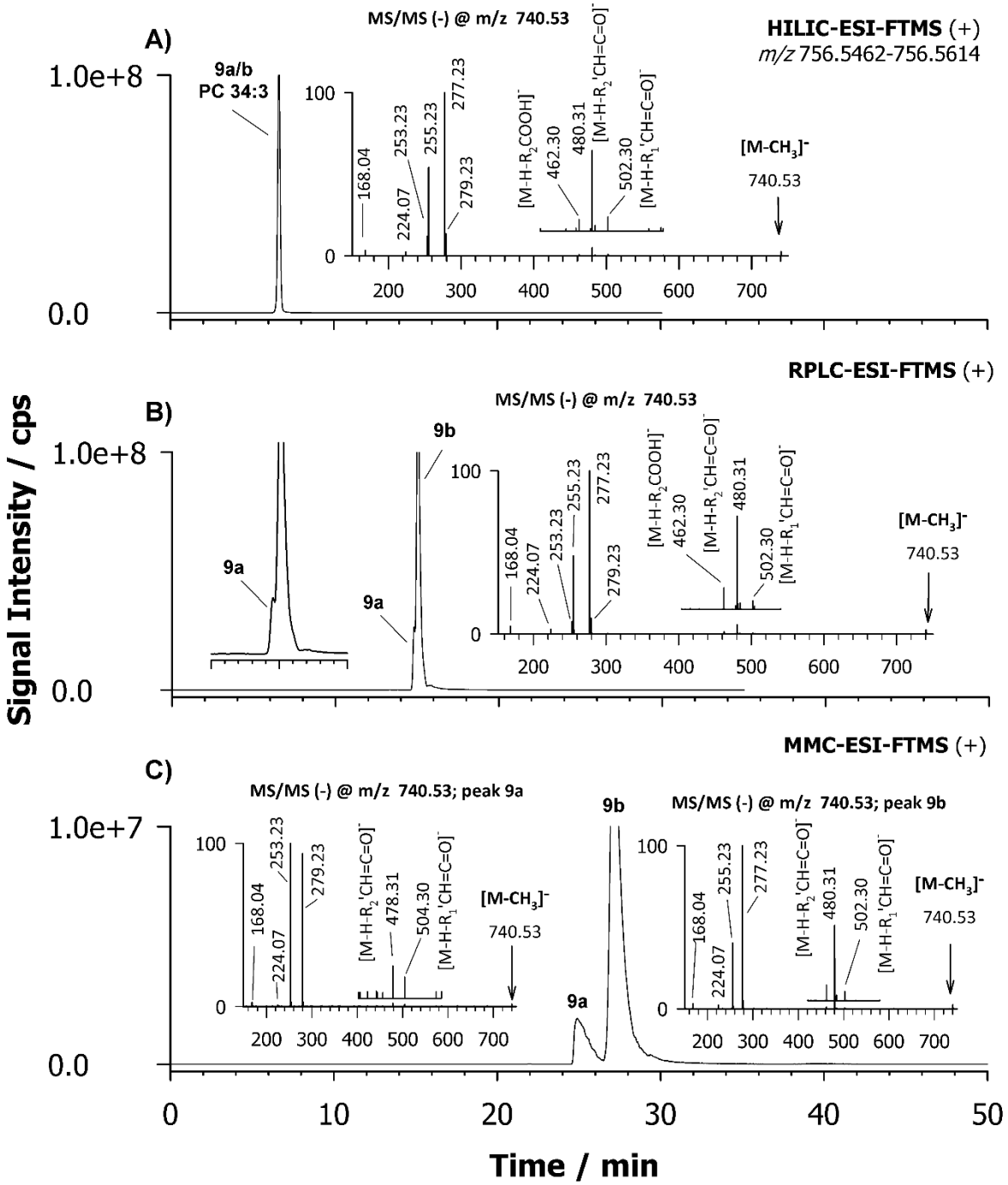

593
594

595 Figure 5
596
597

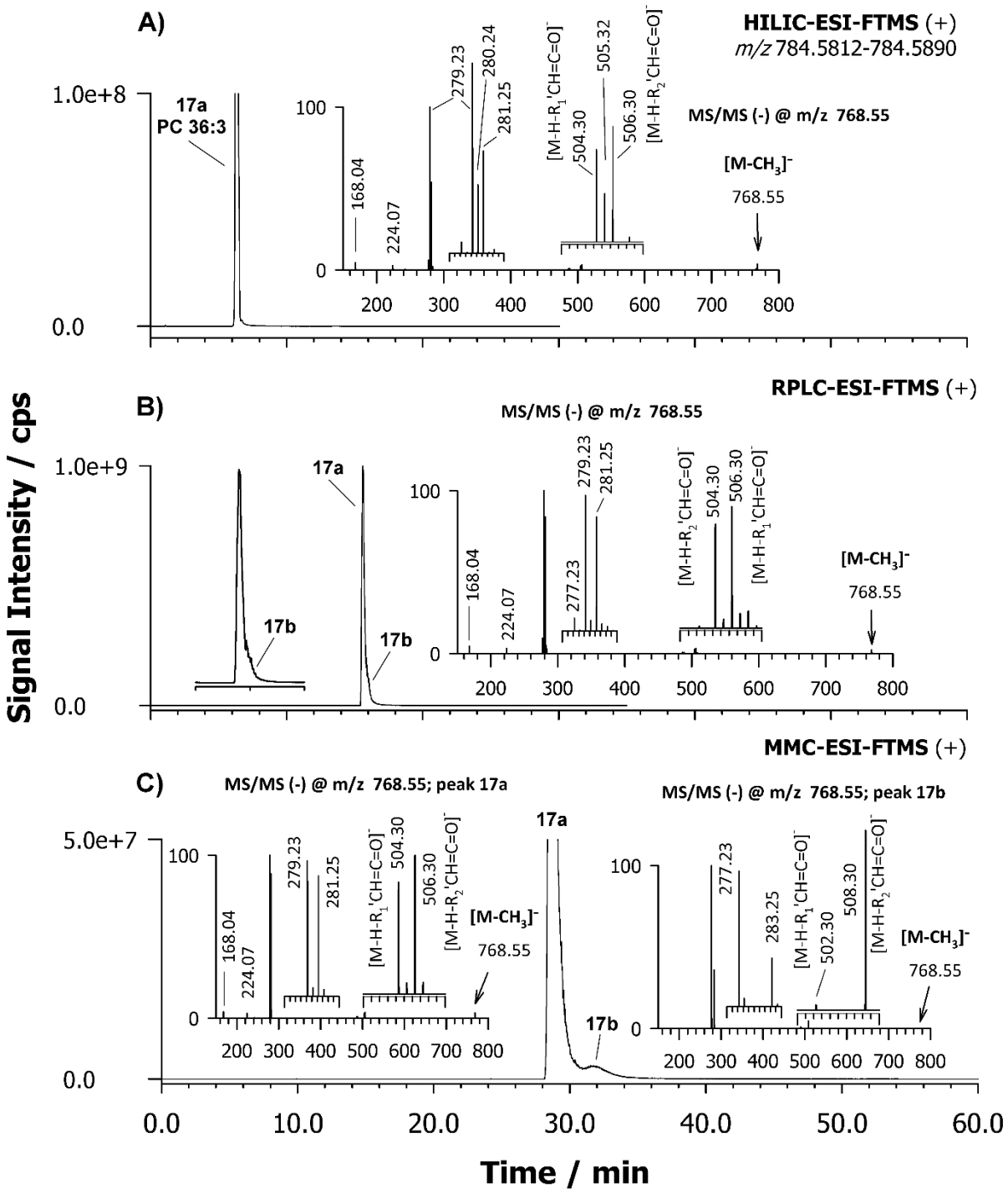

598